

Multiple Metamagnetic Transitions in the Magnetic Refrigerant $\text{La}(\text{Fe}, \text{Si})_{13}\text{H}_x$

Julia Lyubina,^{*} Konstantin Nenkov, Ludwig Schultz, and Oliver Gutfleisch

IFW Dresden, Institute for Metallic Materials, P.O. Box 270016, D-01171, Dresden, Germany

(Received 29 May 2008; published 22 October 2008)

The effect of hydrostatic pressure on thermally and field-induced first-order magnetic phase transitions is studied in the $\text{La}(\text{Fe}, \text{Si})_{13}$ -type compounds. A peculiar series of consecutive field-induced transitions is realized using a distinct combination of hydrostatic pressure and negative pressure created by the interstitial insertion of hydrogen. The pressure-induced discontinuous magnetization jumps result in an enhanced cooling power, thus opening up the possibility to exploit in full the magnetocaloric potential of this compound class.

DOI: [10.1103/PhysRevLett.101.177203](https://doi.org/10.1103/PhysRevLett.101.177203)

PACS numbers: 75.30.Kz, 75.30.Sg

Magnetic refrigeration is based on the magnetocaloric effect (MCE), which is the emission or absorption of heat in a magnetic material in response to a changing magnetic field. The MCE arises due to a change in the entropy caused by the coupling of the magnetic spin system to the magnetic field. Under adiabatic conditions, the magnetic entropy variation is compensated by a temperature change. The two parameters, the adiabatic temperature change ΔT_{ad} and the magnetic entropy change ΔS_M , a measure of the material's cooling power, are used for the evaluation of the MCE [1,2]. For conventional applications, where a magnetic field of about 2 T should be produced by permanent magnets, it is desirable to have the largest entropy change in the smallest volume. Recently, several materials with a so-called giant MCE have been discovered, such as $\text{Gd}_5\text{Si}_2\text{Ge}_2$, MnAs , $\text{Mn}_{1-x}\text{Fe}_x\text{As}$, Ni_2MnSn , and $(\text{Mn}, \text{Fe})_2(\text{P}, \text{As})$ - and $\text{La}(\text{Fe}, \text{Si})_{13}$ -type compounds [3–8]. In all of these materials, a first-order magnetic phase transition occurs near room temperature. The transition gives rise to an abrupt change of the magnetization M near the transition point, which, in turn, results in a large magnetic entropy change, as follows from the equation based on the Maxwell relation

$$\Delta S_M(T, H) = \int_0^H (\partial M / \partial T)_H dH, \quad (1)$$

where T and H are the temperature and the applied magnetic field, respectively.

$\text{La}(\text{Fe}, \text{Si})_{13}$ -type compounds and their hydrides have the potential of becoming the favorite working material for a future near-room-temperature magnetic refrigeration technology, as they satisfy to a great extent demands posed on the magnetic and nonmagnetic properties of active magnetic coolants [9,10]. The giant MCE in $\text{LaFe}_{13-x}\text{Si}_x$ ($x \leq 1.6$) is associated with the thermally induced first-order phase transition from the paramagnetic to the ferromagnetic state at temperatures around 200 K [3]. Additionally, above the Curie temperature T_c , an itinerant-electron metamagnetic (IEM) transition is induced by an external magnetic field. The IEM transition occurs due to the change of

the density of states at the Fermi level $N(E_F)$ under the action of the magnetic field. Both transitions to the ferromagnetic state are accompanied by a sizable volume change of about 1% [11]. The occurrence of the first-order magnetic transitions implies the existence of at least two minima in the free energy of $\text{LaFe}_{13-x}\text{Si}_x$, regarded as a function of magnetic moment [12]. Recent electronic structure calculations have demonstrated that several shallow minima and maxima are present in the total energy versus the spin-moment $E(m)$ curve of $\text{LaFe}_{13-x}\text{Si}_x$ and the transition to the ferromagnetic state involves a series of consecutive transitions [13], not yet observed experimentally. The extrema in the theoretical total energy profile are very sensitive to the lattice parameter of the $\text{La}(\text{Fe}, \text{Si})_{13}$ phase.

In real materials, the lattice parameter can be modified “physically” by applying external pressure or “chemically” via the addition of substitutional or interstitial alloying elements. The application of hydrostatic pressure to the $\text{La}(\text{Fe}, \text{Si})_{13}$ compounds reduces the volume and leads to a significant decrease of the Curie temperature [11]. On the other hand, the substitution of, e.g., Co and Si atoms for Fe or the insertion of hydrogen atoms produces a negative pressure effect (the volume increases) and leads to a rise in the Curie temperature [3,10,14,15], which is desired for a magnetic refrigerant operating close to room temperature. In the $\text{La}(\text{Fe}, \text{Co})_{13-x}\text{Si}_x$ compounds, the substitution of Co for Fe and the increase of Si concentration x above 1.6 result in the change of the order of the magnetic phase transition from first to second and in the disappearance of the IEM transition. In contrast to Si- and Co-substituted LaFe_{13} , the insertion of hydrogen into the $\text{La}(\text{Fe}, \text{Si})_{13}$ compound does not lead to a change of the transition type: The paramagnetic-to-ferromagnetic transition remains of first order [3,10]. Nonetheless, the hydrogen uptake is expected to produce not only a volumetric effect but also to modify the bonding between atoms and to change the position of the Fermi level [16].

In the present work, the interplay between the opposite effects produced by hydrogen uptake and external pressure is studied in melt-spun and annealed $\text{La}(\text{Fe}, \text{Si})_{13}$ -based

materials. Because of the strong dependence of exchange and magnetoelastic interaction on the interatomic distance, hydrostatic pressure is a useful tool for elucidating the mechanism of first-order transitions. Moreover, significant pressure-induced changes in the magneto-responsive characteristics have been reported to enhance the MCE in the MnAs (Ref. [17]) and $\text{Tb}_5\text{Si}_2\text{Ge}_2$ (Ref. [18]) compounds.

An arc-melted $\text{LaFe}_{11.57}\text{Si}_{1.43}$ alloy was rapidly quenched using a melt spinning technique [19] at a speed of 30 m/s. The as-spun ribbons were annealed at 1323 K for 1 h under argon followed by quenching in water. Hydrogenation of the melt-spun and annealed ribbons was carried out at 673 K in 5 bar hydrogen gas. The hydrogen content in $\text{LaFe}_{11.57}\text{Si}_{1.43}\text{H}_x$ was determined by hot extraction to be $x = 1.64$. The structure of the samples was investigated by x-ray diffraction ($\text{CoK}\alpha$ radiation). Rietveld refinement (X'PERT PLUS software) was used for a quantitative phase analysis and for lattice constant determination. Magnetization measurements were carried out using a superconducting quantum interference device magnetometer (Quantum Design MPMS-XL) in fields up to 7 T. Values of the magnetization were normalized to the x-ray volume at ambient conditions. Hydrostatic pressure was applied to samples placed in a piston clamp pressure cell. The pressure inside the cell was determined *in situ* by measuring a shift of the superconducting transition temperature of Sn. The Curie temperature T_c was determined by the Belov-Goryaga method [20] (also known as the Arrot plot [21]) and agrees well with the transition onset in the temperature dependence of the magnetization measured at a field of 10 mT. The magnetic entropy change ΔS_M was calculated from magnetization isotherms $M(H)$ by numerical integration of Eq. (1).

Annealed $\text{LaFe}_{11.57}\text{Si}_{1.43}$ ribbons are of cubic NaN_{13} -type structure (space group $Fm\bar{3}c$) with a small amount of a secondary α -Fe phase (5 wt %). Hydrogenation of the $\text{LaFe}_{11.57}\text{Si}_{1.43}$ compound does not modify the phase composition and the crystal symmetry of the 1:13 phase but leads to lattice expansion. In the $\text{LaFe}_{11.57}\text{Si}_{1.43}\text{H}_{1.64}$ hydride, the lattice constant of the 1:13 phase is $a = (11.605 \pm 0.001) \text{ \AA}$, and the lattice expansion as compared to the parent $\text{LaFe}_{11.57}\text{Si}_{1.43}$ compound is $\Delta a/a = 1.07\%$.

Figure 1(a) shows the temperature variation of the magnetization for $\text{LaFe}_{11.57}\text{Si}_{1.43}$ with and without applied hydrostatic pressure p . At ambient pressure, the Curie temperature T_c of 202 K has been determined for $\text{LaFe}_{11.57}\text{Si}_{1.43}$. Under pressure, a linear shift of T_c to lower temperatures at the rate of $d \ln(T_c)/dp \approx -0.11 \text{ kbar}^{-1}$ is observed, and the width of the thermally induced paramagnetic-to-ferromagnetic transition increases. While the magnitude of the magnetization measured in a low field of 10 mT varies irregularly with applied pressure [22], the magnetization at lower temperatures measured in 5 T decreases only slightly with increasing pressure (inset in Fig. 1). The significant reduction in the magnetization at

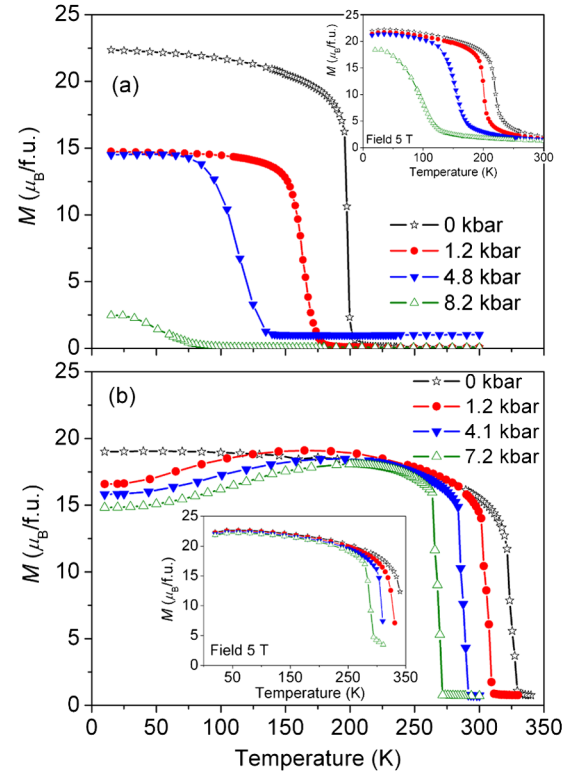


FIG. 1 (color online). The effect of applied hydrostatic pressure on the magnetization M measured on cooling in an external magnetic field of 10 mT for (a) $\text{LaFe}_{11.57}\text{Si}_{1.43}$ and (b) $\text{LaFe}_{11.57}\text{Si}_{1.43}\text{H}_{1.64}$. Inset: The magnetization in a magnetic field of 5 T.

a pressure of 8.2 kbar may be attributed to the incompleteness of the transformation.

Figure 2(a) shows the field dependence of the magnetization for $\text{LaFe}_{11.57}\text{Si}_{1.43}$ near the Curie temperature for various pressures. Characteristic S-shaped magnetization curves, indicative of the field-induced IEM transition, are observed above T_c at ambient pressure. With increasing pressure, the IEM transition, sharp at zero pressure, is gradually broadened over a wider magnetic field interval and the field hysteresis increases. The hysteresis, a fingerprint of the first-order phase transition, persists at temperatures below T_c [Fig. 2(a)].

Hydrogen insertion into the parent $\text{LaFe}_{11.57}\text{Si}_{1.43}$ compound leads to an increase of T_c to 329 K, which is reduced upon further pressure application [Fig. 1(b)]. In the $\text{LaFe}_{11.57}\text{Si}_{1.43}\text{H}_{1.64}$ hydride, the reduction of T_c with hydrostatic pressure can be well described by a quadratic fit $T_c(p) = (325.6 - 10.4p + 0.41p^2) \text{ K}$, and the linear term in the fit corresponds to $d \ln(T_c)/dp \approx -0.03 \text{ kbar}^{-1}$. The rate of the T_c reduction in the $\text{LaFe}_{11.57}\text{Si}_{1.43}\text{H}_{1.64}$ hydride is thus significantly lower as compared to the parent $\text{LaFe}_{11.57}\text{Si}_{1.43}$ compound. This indicates an important role of electron transfer caused by the hydrogen insertion. Under hydrostatic pressure, the thermally induced paramagnetic-to-ferromagnetic transition remains sharp,

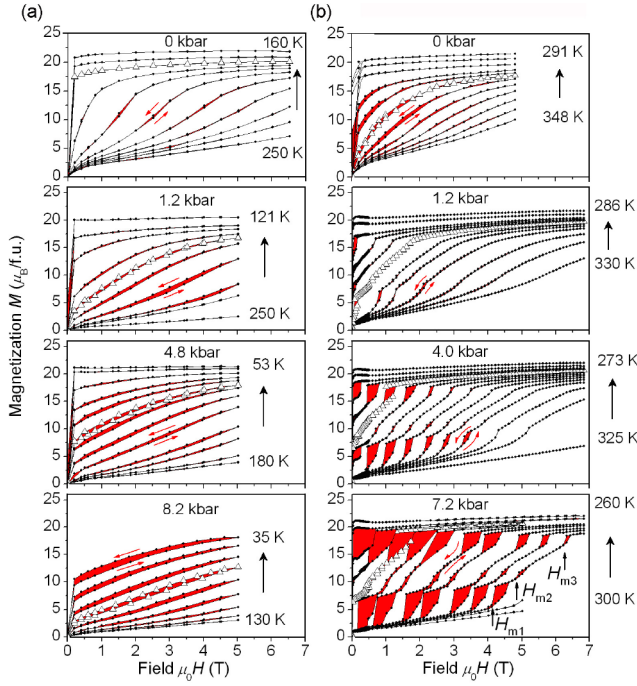


FIG. 2 (color online). Magnetization isotherms in the vicinity of the Curie temperature T_c at various pressures for (a) $\text{LaFe}_{11.57}\text{Si}_{1.43}$ and (b) $\text{LaFe}_{11.57}\text{Si}_{1.43}\text{H}_{1.64}$. Arrows indicate the direction of temperature and magnetic field change. Open triangles mark magnetization curves at T_c . H_{mi} indicates the critical field for the i th metamagnetic transition.

and the temperature dependence of the magnetization measured in a low magnetic field of 10 mT reveals a maximum [Fig. 1(b)], while the magnetization in 5 T increases gradually with decreasing temperature [Fig. 1(b), inset].

In the $\text{LaFe}_{11.57}\text{Si}_{1.43}\text{H}_{1.64}$ hydride, the IEM transition at zero applied pressure is not as sharp as that in the parent $\text{LaFe}_{11.57}\text{Si}_{1.43}$ compound [Fig. 2(b)]. A clear hysteresis in the field dependence of the magnetization is present above and below T_c . On applying pressure, not a single but a series of consecutive transitions takes place. At $p = 1.2$ kbar, three peaks in the derivative dM/dH (not shown) indicate the occurrence of three magnetic transitions at temperatures above T_c , while at zero pressure a single broad dM/dH peak is observed (not shown). At pressures above 1.2 kbar, the transitions are more distinct, and the field hysteresis increases [Fig. 2(b)]. The critical field of all three metamagnetic transitions H_{mi} (defined as a field where $d^2M/dH^2 = 0$) increases with increasing temperature at essentially the same rate (Fig. 3). In the $\text{LaFe}_{11.57}\text{Si}_{1.43}\text{H}_{1.64}$ hydride, the temperature at which the critical field of the first metamagnetic transition vanishes, $H_{m1}(p, T) = 0$, corresponds to the Curie temperature (Fig. 3). The field-induced transitions at the respective fields H_{m2} and H_{m3} are observed above and below T_c [Fig. 2(b)]. A low temperature limit for the disappearance

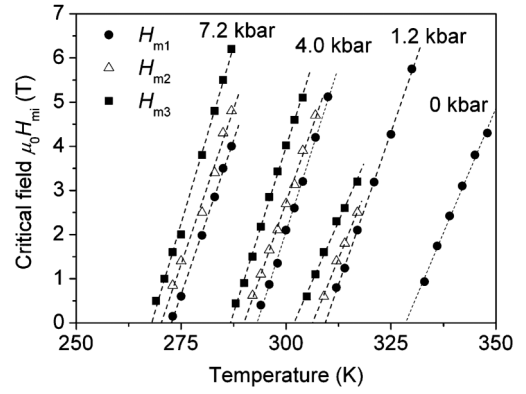


FIG. 3. Temperature dependence of the critical field H_{mi} of the metamagnetic transitions at various pressures in $\text{LaFe}_{11.57}\text{Si}_{1.43}\text{H}_{1.64}$. The dashed lines are linear fits of the experimental data.

of the transitions is a critical temperature T_{mi} , where H_{mi} vanishes (Fig. 3). At higher temperatures, thermal fluctuation effects lead to smearing out of the Fermi level, and the metamagnetic transitions eventually disappear at a critical temperature T_0 . In $\text{LaFe}_{11.57}\text{Si}_{1.43}\text{H}_{1.64}$, $T_0 \approx 325$ K at 4.0 kbar. The exact determination of T_0 , however, requires measurements in high magnetic fields.

The occurrence of three consecutive first-order transitions has been predicted by density-functional electronic structure calculations for $\text{La}(\text{Fe}, \text{Si})_{13}$ without hydrogen [13]. Whereas no discontinuous magnetization jumps are observed experimentally in the parent $\text{LaFe}_{11.57}\text{Si}_{1.43}$ compound, the field hysteresis present in both $\text{LaFe}_{11.57}\text{Si}_{1.43}$ and $\text{LaFe}_{11.57}\text{Si}_{1.43}\text{H}_{1.64}$ below T_c under pressure (Fig. 2) indicates that the mechanism of the transition is apparently of the same origin. In $\text{LaFe}_{11.57}\text{Si}_{1.43}$, the volume reduction due to the application of pressure hinders the IEM transition resulting in a smoother variation of the magnetization [Fig. 2(a)]. Such behavior is consistent with calculation results [13], where the global minimum in the total energy $E(m)$ curve was shown to move to lower magnetic moments m as the volume decreases. Apparently, the insertion of hydrogen modifies the barriers between the minima and their location in the $E(m)$ profile leading to the occurrence of three distinct transitions in $\text{LaFe}_{11.57}\text{Si}_{1.43}\text{H}_{1.64}$ at the fields H_{mi} [Fig. 2(b)]. A further study of the electronic structure is required in order to clarify the contribution of chemical effects and volume expansion associated with the hydrogen insertion.

In the melt-spun $\text{LaFe}_{11.57}\text{Si}_{1.43}$ ribbons, the thermal- and field-broadening effect of pressure on the first-order transition [Figs. 1(a) and 2(a)] is opposite to that in bulk $\text{La}(\text{Fe}, \text{Si})_{13}$, where the transition remains sharp under hydrostatic pressure [11]. The behavior is consistent with the previously observed difference between bulk and thin-ribbon materials [23] and can be attributed to different microstructure in these alloys. In $\text{LaFe}_{11.57}\text{Si}_{1.43}$, the reduction of the field-induced magnetization change dM/dH

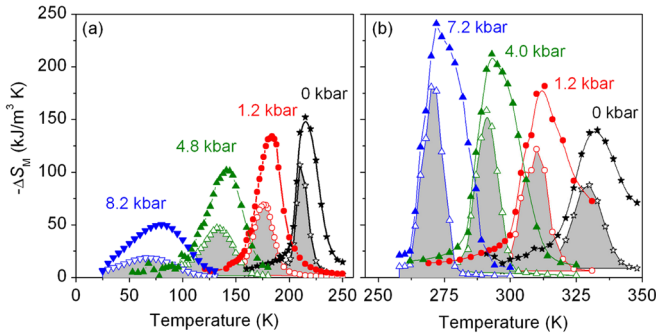


FIG. 4 (color online). Magnetic entropy change ΔS_M as a function of temperature and pressure in (a) $\text{LaFe}_{11.57}\text{Si}_{1.43}$ and (b) $\text{LaFe}_{11.57}\text{Si}_{1.43}\text{H}_{1.64}$. Open and closed symbols correspond to ΔS_M for a field change of 2 and 5 T, respectively.

with pressure leads to the decrease of the maximum entropy change ΔS_{max} from approximately $150 \text{ kJ/m}^3 \text{ K}$ (0 kbar) to $50 \text{ kJ/m}^3 \text{ K}$ (8.2 kbar) for a field change of $\Delta H = 5 \text{ T}$ [Fig. 4(a)]. However, the width of the peak increases, and thus the relative cooling power (RCP), corresponding to the integrated area under the $\Delta S_M(T)$ peak, remains essentially unchanged and equals $1.7(2)$ and $4.3(6) \text{ MJ/m}^3$ for a field change ΔH of 2 and 5 T, respectively. The constancy of RCP is in accordance with a sum rule valid for materials with the constant saturation magnetization [24].

In contrast to the parent compound, the application of pressure to the $\text{LaFe}_{11.57}\text{Si}_{1.43}\text{H}_{1.64}$ hydride leads to a significant increase in both ΔS_{max} [Fig. 4(b)] and RCP, which is due to the discontinuous magnetization change induced during the sequential first-order transitions. The maximum entropy change increases by a factor of 2, and the width of the $\Delta S_M(T)$ peak for a field change of 2 T is reduced from $10.5(3)$ to $7.7(3) \text{ K}$; i.e., the entropy change is concentrated in a narrower temperature range, as the pressure increases from 0 to 7.2 kbar [Fig. 4(b)]. For a field change of 2 T, the RCP increases from $1.3(1) \text{ MJ/m}^3$ (0 kbar) to $1.8(2) \text{ MJ/m}^3$ (7.2 kbar), while the RCP for a field change of 5 T is equal to $3.7(2) \text{ MJ/m}^3$ (4.0 kbar) and $4.4(4) \text{ MJ/m}^3$ (7.2 kbar).

Beyond a fundamental importance of pressure in revealing the mechanism of the first-order transitions, better cooling efficiency of magnetic refrigerators can be achieved when using pressure in combination with the magnetic field [25]. The pressure-induced changes of the magnetic phase transitions in $\text{La}(\text{Fe}, \text{Si})_{13}\text{H}_x$ open up the possibility to increase the cooling power and to widen the working temperature span of this magnetic refrigerant. In order to fully exploit the potential of the $\text{La}(\text{Fe}, \text{Si})_{13}$ -based compounds, it is also appealing to imitate the hydrostatic pressure effect on the magnetism

of the $\text{La}(\text{Fe}, \text{Si})_{13}\text{H}_x$ hydrides, e.g., by substitutional modification.

The authors thank U. Hannemann, M.D. Kuz'min, M. Richter, and T.G. Woodcock for stimulating discussions and critical reading of the manuscript. M. Herrich and B. Gebel are gratefully acknowledged for assistance with the material preparation. This work was supported by the Deutsche Forschungsgemeinschaft (DFG), Contract No. RI 932/4-1.

*Corresponding author.

j.lyubina@ifw-dresden.de

- [1] A. M. Tishin and Y. I. Spichkin, *The Magnetocaloric Effect and Its Applications* (Institute of Physics, Bristol, 2003).
- [2] K. A. Gschneidner, Jr., V. K. Pecharsky, and A. O. Tsokol, *Rep. Prog. Phys.* **68**, 1479 (2005).
- [3] A. Fujita *et al.*, *Phys. Rev. B* **67**, 104416 (2003).
- [4] V. K. Pecharsky and K. A. Gschneidner, Jr., *Phys. Rev. Lett.* **78**, 4494 (1997).
- [5] H. Wada and Y. Tanabe, *Appl. Phys. Lett.* **79**, 3302 (2001).
- [6] A. de Campos *et al.*, *Nature Mater.* **5**, 802 (2006).
- [7] T. Krenke *et al.*, *Nature Mater.* **4**, 450 (2005).
- [8] O. Tegus *et al.*, *Nature (London)* **415**, 150 (2002).
- [9] E. Brück, in *Handbook of Magnetic Materials* Vol. 17, edited by K. H. J. Buschow (North-Holland, Amsterdam, 2008).
- [10] J. Lyubina *et al.*, *J. Magn. Magn. Mater.* **320**, 2252 (2008).
- [11] A. Fujita *et al.*, *Phys. Rev. B* **65**, 014410 (2001).
- [12] H. Yamada, *Phys. Rev. B* **47**, 11 211 (1993).
- [13] M. D. Kuz'min and M. Richter, *Phys. Rev. B* **76**, 092401 (2007).
- [14] X. B. Liu and Z. Altounian, *J. Magn. Magn. Mater.* **264**, 209 (2003).
- [15] A. Yan, K.-H. Müller, and O. Gutfleisch, *J. Alloys Compd.* **450**, 18 (2008).
- [16] G. Wiesinger and G. Hilscher, in *Handbook of Magnetic Materials* Vol. 17, edited by K. H. J. Buschow (Elsevier, Amsterdam, 2008).
- [17] S. Gama *et al.*, *Phys. Rev. Lett.* **93**, 237202 (2004).
- [18] L. Morellon *et al.*, *Phys. Rev. Lett.* **93**, 137201 (2004).
- [19] O. Gutfleisch, A. Yan, and K.-H. Müller, *J. Appl. Phys.* **97**, 10M305 (2005).
- [20] K. P. Belov and A. N. Goryaga, *Fiz. Met. Metalloved.* **2**, 3 (1956).
- [21] A. Arrott, *Phys. Rev.* **108**, 1394 (1957).
- [22] The magnetization at 4.8 kbar does not approach zero above T_c , which is a measurement artifact. The superconducting magnet was not reset prior to this measurement, and the effective field is slightly higher than 10 mT.
- [23] A. Yan, K.-H. Müller, and O. Gutfleisch, *J. Appl. Phys.* **97**, 036102 (2005).
- [24] R. D. McMichael *et al.*, *J. Magn. Magn. Mater.* **111**, 29 (1992).
- [25] A. M. Tishin, *J. Alloys Compd.* **250**, 635 (1997).